Hindawi
Journal of Applied Mathematics
Volume 2022, Article ID 8998193, 9 pages
https://doi.org/10.1155/2022/8998193

Research Article

Barycentric Rational Collocation Method for Nonlinear Heat Conduction Equation

Jin Li

School of Science, Shandong Jianzhu University, Jinan 250101, China

Correspondence should be addressed to Jin Li; lijin@lsec.cc.ac.cn

Received 9 May 2022; Accepted 17 June 2022; Published 30 June 2022

Academic Editor: Saeid Abbasbandy

Nonlinear heat equation solved by the barycentric rational collocation method (BRCM) is presented. Direct linearization method and Newton linearization method are presented to transform the nonlinear heat conduction equation into linear equations. The matrix form of nonlinear heat conduction equation is also obtained. Several numerical examples are provided to valid our schemes.

1. Introduction

In this article, the nonlinear heat conduction equation is considered as

$$\frac{\partial u(x,t)}{\partial t} = c(x,t,u)\frac{\partial^2 u(x,t)}{\partial x^2} + F\left(x,t,u,\frac{\partial u(x,t)}{\partial x}\right), a \le x \le b, t \ge 0, \tag{1}$$

where $F(x,t,u,(\partial u(x,t)/\partial x))$ is the nonlinear term of u and u_x, with initial condition

$$u(x,0) = f(x), a \le x \le b, \tag{2}$$

and the boundary condition

$$u(a,t) = \varphi_1(t) \quad u(b,t) = \varphi_2(t), t \ge 0. \tag{3}$$

Combining (1)–(3), we get nonlinear heat conduction equation.

The linear and nonlinear heat conduction equation is a second-order linear partial differential equation [1–6]. There are analytical and numerical methods to solve the linear/nonlinearheat conduction equation. For the numerical methods, there are the finite difference method, finite element method and boundary element method, the spectral method [7], etc.

The barycentric formula have been obtained by the Lagrange interpolation formula [8–10] and been used to solve Volterra equation and Volterra integro-differential equation [11–14]. Floater and Kai, Klein and Berrut [15–17] have proposed a rational interpolation scheme and get the equidistant node of the barycentric formula. In recent papers, references [18–25] have been extended the barycentric collocation methods to solve initial/boudary value problems and linear/nonlinear problems.

In this paper, the linear barycentric rational collocation method (LBRCM) for nonlinear heat conduction equation is presented. Direct linearization and Newton linearization are presented to transform the nonlinear heat conduction equation into linear equations. The matrix form of linearization scheme for nonlinear heat conduction equation is also obtained.

This paper is organized as follows: in Section 2, the linearization scheme for nonlinear heat conduction equation is given. Direct linearization and Newton linearization are constructed, and then the matrix form of LBRCM is also presented. At last, two numerical examples are listed to illustrate our numerical scheme.

2. Linearization

Direct linearization and Newton linearization are presented to change the nonlinear heat conduction equation into linear equation. By choosing the equidistant nodes and Chebyshev nodes as collocation point to solve the nonlinear heat conduction equation, the direct linearization scheme can be adopted as

$$\frac{\partial u(x,t)}{\partial t} = c(x,t,u_0)\frac{\partial^2 u(x,t)}{\partial x^2} + F\left(x,t,u_0,\frac{\partial u_0(x,t)}{\partial x}\right),$$
$$\frac{\partial u_n(x,t)}{\partial t} = c(x,t,u_{n-1})\frac{\partial^2 u_n(x,t)}{\partial x^2} + F\left(x,t,u_{n-1},\frac{\partial u_{n-1}(x,t)}{\partial x}\right). \tag{4}$$

Newton linearization scheme can be adopted as

$$\frac{\partial u(x,t)}{\partial t} = c(x,t,u)\frac{\partial^2 u(x,t)}{\partial x^2} + F\left(x,t,u_0,\frac{\partial u_0(x,t)}{\partial x}\right)(u-u_0)+\cdots, \tag{5}$$

and then we get the Newton linearization as

$$\frac{\partial u(x,t)}{\partial t} = c(x,t,u)\frac{\partial^2 u(x,t)}{\partial x^2} + F\left(x,t,u_0,\frac{\partial u_0(x,t)}{\partial x}\right)(u-u_0),$$
$$\frac{\partial u_n(x,t)}{\partial t} = c(x,t,u_{n-1})\frac{\partial^2 u_n(x,t)}{\partial x^2} + F\left(x,t,u_{n-1},\frac{\partial u_{n-1}(x,t)}{\partial x}\right)(u_n-u_{n-1}). \tag{6}$$

We partition the interval $[a,b]$ into $a=x_0<x_1<\cdots<x_m=b, h=b-a/m$ and $[0,T]$ into $0=t_0<t_1<\cdots<t_n=T, \tau=T/n$ with $\Omega=[a,b]\times[0,T]$ and $(x_i,t_j), i=0,1,2,\cdots,m; j=0,1,2,\cdots,n$. Then, we have

$$r_{m,n}(x,t)=\sum_{i=0}^{m}\sum_{j=0}^{n} r_i(x)r_j(t)u_{i,j}, \tag{7}$$

where $u_{i,j}=u(x_i,t_j)$ and

$$r_i(x)=\frac{w_i/x-x_i}{\sum_{j=0}^{n}\left(w_j/x-x_j\right)}, r_j(t)=\frac{w_j/t-t_j}{\sum_{j=0}^{m}\left(w_j/t-t_j\right)},$$
$$w_k=\sum_{i\in J_k}(-1)^i\prod_{j=i,j\neq k}^{i+d}\frac{1}{x_k-x_j}, \tag{8}$$

and $J_k=\{i\in I; k-d\le i\le k\}, I=\{0,1,\cdots,n-d\}$.

Taking equation (7) into equation (1), we can get the LBRCM as

$$\sum_{i=0}^{m}\sum_{j=0}^{n} r_i(x)r_j{}'(t)u_{i,j}=c\left(x,t,\sum_{i=0}^{m}\sum_{j=0}^{n} r_i(x)r_j(t)u_{i,j}\right)\sum_{i=0}^{m}\sum_{j=0}^{n} r''{}_i(x)r_j(t)u_{i,j}$$
$$+F\left(x,t,\sum_{i=0}^{m}\sum_{j=0}^{n} r_i(x)r_j(t)u_{i,j},\sum_{i=0}^{m}\sum_{j=0}^{n} r_i'(x)r_j(t)u_{i,j}\right). \tag{9}$$

3. Numerical Examples

In the following, two examples are given to valid our algorithm.

Example 1. Consider

$$\frac{\partial u}{\partial t}=\frac{\partial^2 u}{\partial x^2}+e^{-u}+e^{-2u}, a<x<b; t\ge 0, \tag{10}$$

with

$$u(0,t)=\ln(t+2), u(1,t)=\ln(t+3),$$
$$u(x,0)=\ln(x+2), \tag{11}$$

Its analysis solutions is

$$u(x,t)=\ln(x+t+2). \tag{12}$$

Firstly, direct linearization of nonlinear heat conduction equation is given as

$$\frac{\partial u}{\partial t}=\frac{\partial^2 u}{\partial x^2}+e^{-u_0}+e^{-2u_0}, a<x<b; t>0, \tag{13}$$

with its direct linearization scheme is

$$\frac{\partial u_n}{\partial t}=\frac{\partial^2 u_n}{\partial x^2}+e^{-u_{n-1}}+e^{-2u_{n-1}}, n=1,2,\cdots, \tag{14}$$

and its matrix form is

$$\left[D^{(0,1)}-D^{(2,0)}\right]u_n=e^{-u_{n-1}}+e^{-2u_{n-1}}, \quad n=1,2,\cdots, \tag{15}$$

where

$$D_{ij}^{(m0)}=R_i^{(m)}(x_j), \quad m=1,2, D_{ij}^{(01)}=R_i^{(1)}(t_j), \tag{16}$$

$$D_{ij}^{(10)}=\begin{cases}\dfrac{w_i/w_j}{x_j-x_i}, & j\neq i,\\ -\sum\limits_{i\neq j} D_{ji}^{(10)}, & j=i,\end{cases} \quad D_{ji}^{(20)}=\begin{cases}2D_{ji}^{(10)}\left(D_{ji}^{(10)}-\dfrac{1}{x_j-x_i}\right), & j\neq i,\\ -\sum\limits_{i\neq j} D_{ji}^{(20)}, & j=i,\end{cases} \tag{17}$$

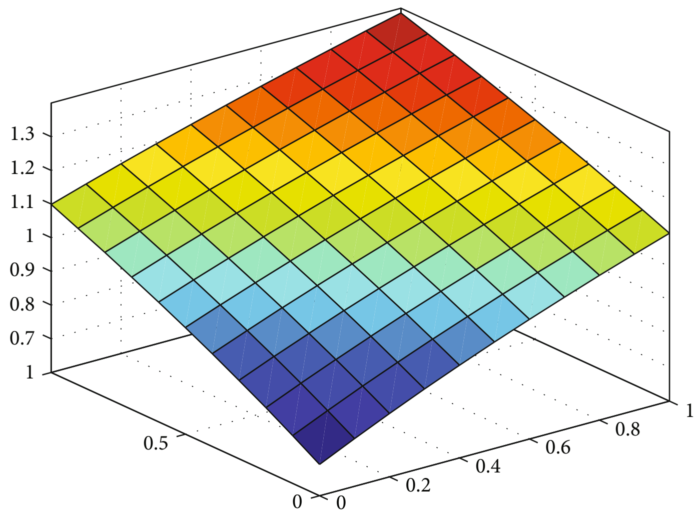

Figure 1: Analysis solutions of $u(x,t) = \ln(x + t + 2)$.

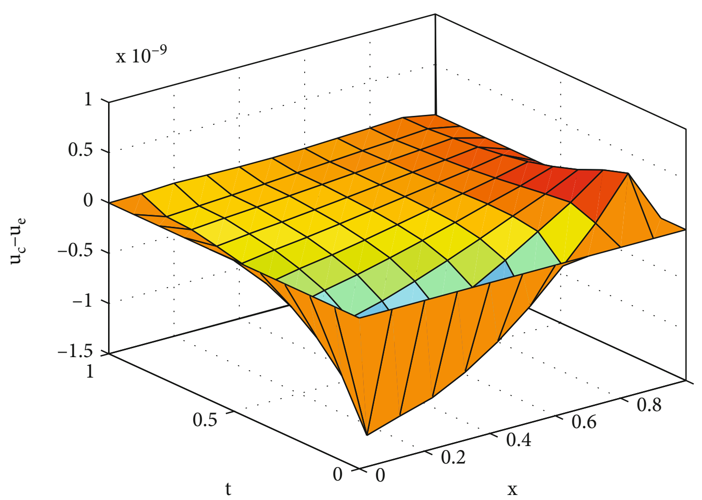

Figure 2: Errors of equidistant nodes for LBRCM with $m = n = 10$, $d_1 = d_2 = 7$.

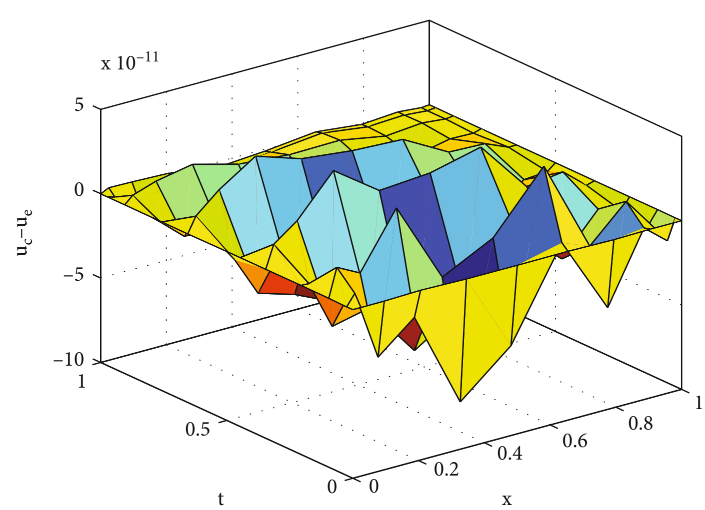

Figure 3: Errors of Chebyshev nodes for LBRCM with $m = n = 10$, $d_1 = d_2 = 7$.

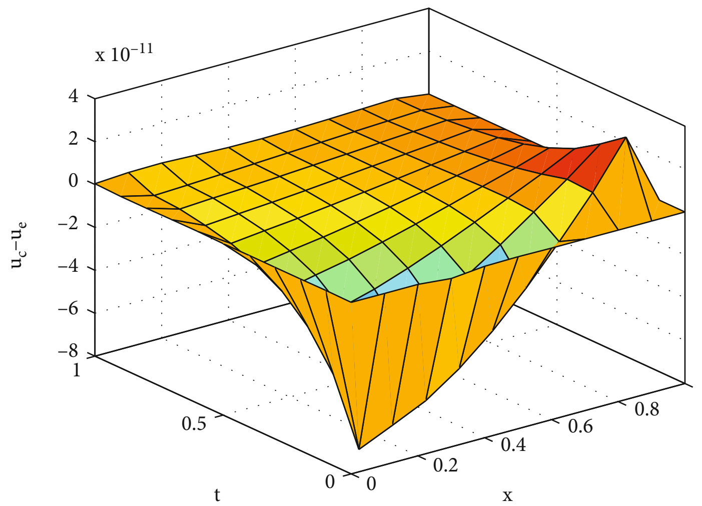

Figure 4: Errors of equidistant nodes for BLCM with $m = n = 10$.

$$D_{ij}^{(01)} = \begin{cases} \dfrac{w_i/w_j}{t_j - t_i}, & j \neq i, \\ -\sum\limits_{i\neq j} D_{ji}^{(01)}, & j = i. \end{cases} \tag{18}$$

In Figure 1, the analysis solution $u(x,t) = \ln(x + t + 2)$ is presented. In the following Figures 2 and 3, errors of equidistant nodes and Chebyshev nodes for LBRCM with $m = n = 10, d_1 = d_2 = 7$ are given, respectively; from the figure, we know that the accuracy of Chebyshev nodes is higher than equidistant nodes.

In the following Figures 4 and 5, errors of equidistant nodes and Chebyshev nodes for BLCM with $m = n = 10$ are given, respectively; from the figure, we know that the accuracy of Chebyshev nodes is also higher than equidistant nodes.

In Tables 1 and 2, the errors of direct linearization scheme by LBRCM with equidistant nodes for x and t are presented.

In Tables 3 and 4, the errors of the LBRCM with Chebyshev nodes for x and t are presented.

Secondly, Newton linearization of nonlinear heat conduction equation is given as

$$\frac{\partial u}{\partial t} = \frac{\partial^2 u}{\partial x^2} + \left(e^{-u_0} + e^{-2u_0}\right)(u - u_0), a < x < b\,; t \geq 0, \tag{19}$$

with its Newton linearization scheme that is

$$\frac{\partial u_n}{\partial t} = \frac{\partial^2 u_n}{\partial x^2} + \left(e^{-u_{n-1}} + e^{-2u_{n-1}}\right)(u_n - u_{n-1}), n = 1, 2, \cdots, \tag{20}$$

and its matrix form is

$$\left[D^{(0,1)} - D^{(2,0)} + \operatorname{diag}\left(e^{-u_{n-1}} + 2e^{-2u_{n-1}}\right)\right] u_n = e^{-u_{n-1}} + e^{-2u_{n-1}} + \left(e^{-u_{n-1}} + 2e^{-2u_{n-1}}\right) \circ u_{n-1}, n = 1, 2, \cdots, \tag{21}$$

where $D^{(0,1)}$ and $D^{(2,0)}$ are defined as (16).

In Tables 5 and 6, the errors of Newton linearization scheme by LBRCM with equidistant nodes for x and t are presented.

In Tables 7 and 8, the errors of Newton linearization by LBRCM with Chebyshev nodes for x and t are presented.

From the table above, we know that the accuracy of Newton linearization scheme is higher than direct linearization scheme.

Example 2. Consider

$$\frac{\partial u}{\partial t} = \alpha \frac{\partial^2 u}{\partial x^2} - u \frac{\partial u}{\partial x} + f(x,t), a < x < b\,; t > 0, \tag{22}$$

with the condition

$$f(x,t) = \sin(6\pi x)\left(36\pi^2 \cos(t) - \sin(t) + 6\pi \cos(6\pi x) \cos^2(t)\right),$$
$$u(x,0) = \sin(6\pi x), u(0,t) = 0. \tag{23}$$

Its analysis solutions is

$$u(x,t) = \cos(t) \sin(6\pi x). \tag{24}$$

In this example, direct linearization scheme is presented

$$\frac{\partial u}{\partial t} = \frac{\partial^2 u}{\partial x^2} - u \frac{\partial u}{\partial x} + e^{-u_0} + e^{-2u_0}, a < x < b\,; t > 0, \tag{25}$$

Table 1: Errors of the LBRCM with $d_2 = 7$ at $t = 1$ for equidistant nodes.

m, n	$d_1 = 1$	h^α	$d_1 = 2$	h^α	$d_1 = 3$	h^α	$d_1 = 4$	h^α
8, 8	5.8782e-04		1.4718e-05		6.2224e-06		5.3762e-07	
16, 16	1.8139e-04	1.6963	1.9147e-06	2.9424	3.6861e-07	4.0773	2.1906e-08	4.6172
32, 32	5.4855e-05	1.7254	2.5010e-07	2.9365	2.3239e-08	3.9874	7.8080e-10	4.8102
64, 64	1.6239e-05	1.7561	3.2280e-08	2.9538	1.5064e-09	3.9474	8.2417e-11	3.2439

Table 2: Errors of the LBRCM with $d_1 = 7$ at $t = 1$ for equidistant nodes.

m, n	$d_2 = 1$	τ^α	$d_2 = 2$	τ^α	$d_2 = 3$	τ^α	$d_2 = 4$	τ^α
8, 8	9.5811e-04		1.7102e-05		5.4941e-06		3.4075e-07	
16, 16	5.2156e-04	0.8774	5.2640e-06	1.7000	8.0961e-07	2.7626	3.2948e-08	3.3704
32, 32	2.3682e-04	1.1390	1.3002e-06	2.0175	9.8320e-08	3.0417	2.2777e-09	3.8545
64, 64	9.5433e-05	1.3112	2.8040e-07	2.2132	1.0531e-08	3.2228	1.2354e-10	4.2045

Table 3: Errors of the LBRCM with $d_2 = 7$ at $t = 1$ for Chebyshev nodes.

m, n	$d_1 = 1$	h^α	$d_1 = 2$	h^α	$d_1 = 3$	h^α	$d_1 = 4$	h^α
8, 8	1.3717e-03		1.5290e-05		6.3486e-06		1.6112e-07	
16, 16	3.3177e-04	2.0477	1.2090e-06	3.6607	8.3105e-08	6.2554	3.2477e-09	5.6326
32, 32	7.7738e-05	2.0935	7.4116e-08	4.0279	2.5853e-09	5.0065	1.5222e-09	—
64, 64	8.4472e-05	—	4.3077e-06	—	5.6046e-06	—	2.0141e-06	—

Table 4: Errors of the LBRCM with $d_1 = 7$ at $t = 1$ for Chebyshev nodes.

m, n	$d_2 = 1$	τ^α	$d_2 = 2$	τ^α	$d_2 = 3$	τ^α	$d_2 = 4$	τ^α
8, 8	5.7527e-04		8.8997e-06		1.7666e-06		8.3203e-08	
16, 16	1.4898e-04	1.9492	1.2899e-06	2.7865	1.5065e-07	3.5517	5.5006e-09	3.9190
32, 32	3.5408e-05	2.0729	1.5959e-07	3.0148	9.1369e-09	4.0433	2.7123e-10	4.3420
64, 64	8.7961e-06	2.0091	2.9251e-08	2.4478	1.2933e-07	—	1.2630e-07	—

Table 5: Errors of the LBRCM with $d_2 = 7$ at $t = 1$ for equidistant nodes.

m, n	$d_1 = 1$	τ^α	$d_1 = 2$	h^α	$d_1 = 3$	h^α	$d_1 = 4$	h^α
8, 8	9.5811e-04		1.7102e-05		5.4941e-06		3.4075e-07	
16, 16	5.2156e-04	0.8774	5.2640e-06	1.7000	8.0961e-07	2.7626	3.2949e-08	3.3704
32, 32	2.3682e-04	1.1390	1.3002e-06	2.0175	9.8318e-08	3.0417	2.2716e-09	3.8584
64, 64	9.5433e-05	1.3112	2.8038e-07	2.2132	1.0422e-08	3.2378	1.8173e-10	3.6439

Table 6: Errors of the LBRCM with $d_1 = 7$ at $t = 1$ for equidistant nodes.

m, n	$d_2 = 1$	τ^α	$d_2 = 2$	τ^α	$d_2 = 3$	τ^α	$d_2 = 4$	τ^α
8, 8	5.8782e-04		1.4718e-05		6.2224e-06		5.3762e-07	
16, 16	1.8139e-04	1.6963	1.9147e-06	2.9424	3.6861e-07	4.0773	2.1906e-08	4.6172
32, 32	5.4855e-05	1.7254	2.5009e-07	2.9366	2.3236e-08	3.9877	7.7787e-10	4.8157
64, 64	1.6239e-05	1.7561	3.2275e-08	2.9540	1.4867e-09	3.9661	5.7909e-11	3.7477

Table 7: Errors of the LBRCM with $d_2 = 7$ at $t = 1$ for Chebyshev nodes.

m, n	$d_1 = 1$	h^α	$d_1 = 2$	h^α	$d_1 = 3$	h^α	$d_1 = 4$	h^α
8, 8	5.7527e-04		8.8997e-06		1.7666e-06		8.3204e-08	
16, 16	1.4898e-04	1.9492	1.2899e-06	2.7865	1.5065e-07	3.5517	5.5041e-09	3.9181
32, 32	3.5408e-05	2.0729	1.5957e-07	3.0150	8.8804e-09	4.0844	1.7617e-10	4.9654
64, 64	8.7936e-06	2.0096	2.4359e-08	2.7116	5.8007e-08	—	2.0160e-07	—

Table 8: Errors of the LBRCM with $d_1 = 7$ at $t = 1$ for Chebyshev nodes.

m, n	$d_2 = 1$	τ^α	$d_2 = 2$	τ^α	$d_2 = 3$	τ^α	$d_2 = 4$	τ^α
8, 8	1.3717e-03		1.5290e-05		6.3486e-06		1.6112e-07	
16, 16	3.3177e-04	2.0477	1.2090e-06	3.6607	8.3105e-08	6.2554	3.2477e-09	5.6326
32, 32	7.7738e-05	2.0935	7.4196e-08	4.0263	2.2857e-09	5.1842	4.6534e-10	2.8031
64, 64	8.1984e-05	—	5.4975e-07	—	7.8881e-06	—	9.1447e-07	—

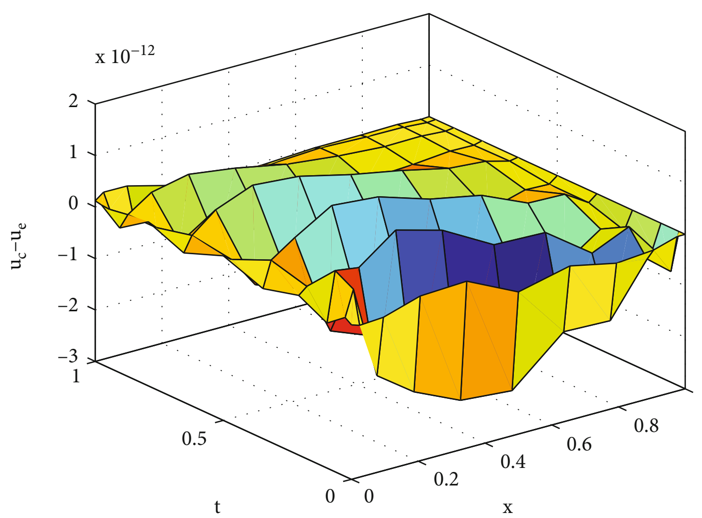

Figure 5: Errors of Chebyshev nodes for BLCM with $m = n = 10$.

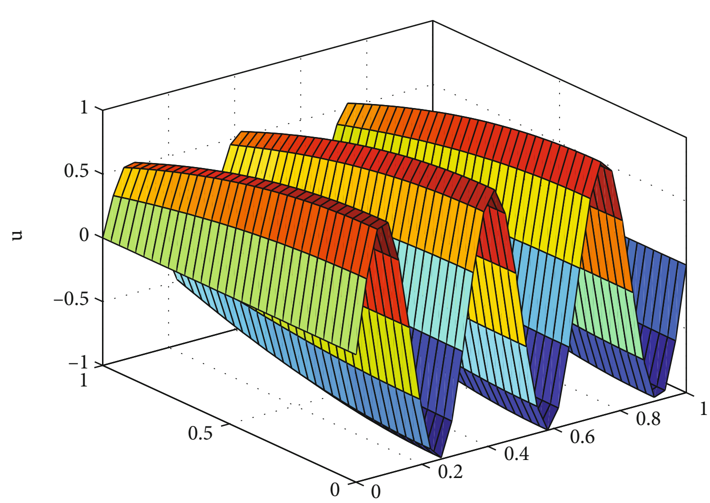

Figure 6: Analysis solutions of $u(x, t) = \cos(t) \sin(6\pi x)$.

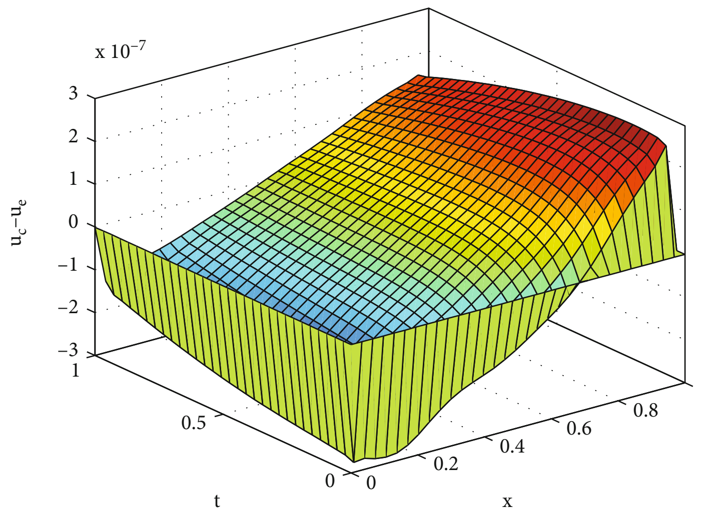

FIGURE 7: Errors of equidistant nodes for LBRCM with $m = n = 31, d_1 = d_2 = 15$.

TABLE 9: Errors of the LBRCM with $d_2 = 7$ at $t = 1$ for equidistant nodes.

m, n	$d_1 = 1$	h^α	$d_1 = 2$	h^α	$d_1 = 3$	h^α	$d_1 = 4$	h^α
8, 8	5.0725e-01		1.6979e+00		7.4870e+00		5.0517e+01	
16, 16	3.8989e-02	3.7016	1.3298e-01	3.6745	1.0527e-01	6.1523	3.6951e-02	10.417
32, 32	8.2371e-03	2.2428	1.4130e-02	3.2344	1.9625e-03	5.7452	3.7448e-03	3.3027
64, 64	2.3338e-03	1.8194	1.6289e-03	3.1168	4.9679e-06	8.6259	1.2120e-04	4.9495

TABLE 10: Errors of the LBRCM with $d_1 = 7$ at $t = 1$ for equidistant nodes.

m, n	$d_2 = 2$	τ^α	$d_2 = 3$	τ^α	$d_2 = 4$	τ^α		
8, 8	3.0358e+01		3.5536e+01		3.2379e+01		3.1088e+01	
16, 16	4.6120e-02	9.3625	4.5581e-02	9.6066	4.5403e-02	9.4781	4.5327e-02	9.4218
32, 32	7.1933e-04	6.0026	7.0368e-04	6.0174	7.0268e-04	6.0138	7.0221e-04	6.0123
64, 64	2.0118e-05	5.1601	9.7053e-07	9.5019	9.6556e-07	9.5073	9.6539e-07	9.5066

TABLE 11: Errors of the LBRCM with $d_2 = 7$ at $t = 1$ for Chebyshev nodes.

m, n	$d_1 = 1$	h^α	$d_1 = 2$	h^α	$d_1 = 3$	h^α	$d_1 = 4$	h^α
8, 8	3.8779e+00		3.7472e+00		3.6747e+00		3.6317e+00	
16, 16	7.1754e-03	9.0780	7.0233e-03	9.0594	7.0547e-03	9.0248	6.9460e-03	9.0303
32, 32	3.3421e-05	7.7462	7.5693e-06	9.8578	7.9371e-06	9.7957	8.8251e-06	9.6203
64, 64	1.3473e-05	1.3107	4.5503e-08	7.3780	4.4917e-09	10.787	8.2779e-09	10.058

TABLE 12: Errors of the LBRCM with $d_1 = 7$ at $t = 1$ for Chebyshev nodes.

m, n	$d_2 = 1$	τ^α	$d_2 = 2$	τ^α	$d_2 = 3$	τ^α	$d_2 = 4$	τ^α
8, 8	4.5490e+00		2.1362e+00		2.1145e+00		2.6899e+00	
16, 16	7.7786e-02	5.8699	3.0474e-02	6.1313	1.5449e-02	7.0967	9.2472e-03	8.1843
32, 32	1.6150e-02	2.2679	2.5803e-03	3.5620	5.0884e-04	4.9241	2.0372e-04	5.5043
64, 64	1.1859e-02	0.4456	1.1541e-03	1.1607	2.1401e-04	1.2495	4.4209e-05	2.2042

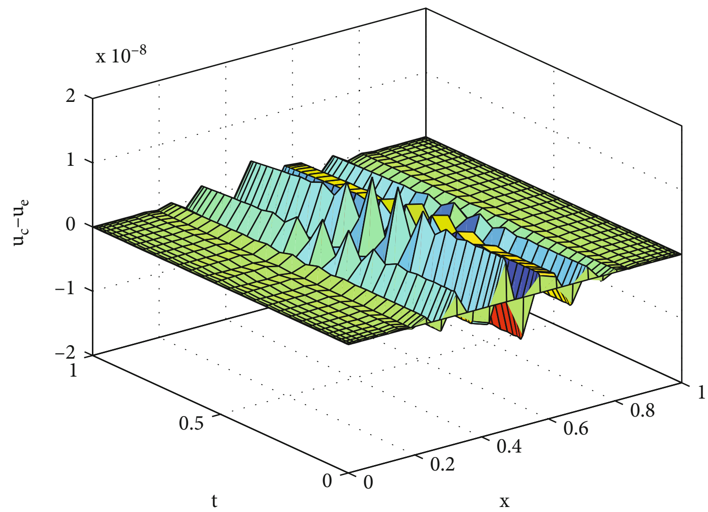

FIGURE 8: Errors of Chebyshev nodes for LBRCM with $m = n = 31$, $d_1 = d_2 = 15$.

with its direct linearization scheme is

$$\frac{\partial u_n}{\partial t} = \frac{\partial^2 u_n}{\partial x^2} - u_{n-1}\frac{\partial u_n}{\partial x} + e^{-u_{n-1}} + e^{-2u_{n-1}}, n = 1, 2, \cdots, \quad (26)$$

and its matrix form is

$$\left[D^{(0,1)} - \alpha D^{(2,0)} + \text{diag}\,(u_{n-1})D^{(1,0)}\right]u_n = F, n = 1, 2, \cdots, \quad (27)$$

where $D^{(0,1)}$ and $D^{(2,0)}$ are defined as (16).

In Figure 6, the analysis solution $u(x, t) = \cos(t)\sin(6\pi x)$ is presented. In the following Figures 7 and 8, errors of equidistant nodes and Chebyshev nodes for LBRCM with $m = n = 31$, $d_1 = d_2 = 15$ are given, respectively; from the figure, we know that the accuracy of Chebyshev nodes is higher than equidistant nodes.

In Tables 9 and 10, the errors of direct linearization by LBRCM with equidistant nodes for x and t are presented.

In Tables 11 and 12, the errors of direct linearization by LBRCM with Chebyshev nodes for x and t are presented.

4. Concluding Remarks

The nonlinear heat conduction equation is solved by LBRCM with direct linearization scheme and Newton linearization scheme, different from the finite difference methods with the time variable computed separately, while the LBRCM can get the space variable and time variable simultaneously. The matrix form of LBRCM with direct linearization scheme and Newton linearization scheme is given from the corresponding scheme, and numerical results are given to valid our scheme. In the table, the convergence of LBRCM for equidistant nodes and Chebyshev nodes has been given, while the theorem analysis of direct linearization scheme and Newton linearization scheme is out of goal in this paper which will be given in the near future.

Data Availability

The data that support the findings of this study are available from the corresponding author upon reasonable request.

Conflicts of Interest

The author declares that he/she has no conflicts of interest.

Acknowledgments

The work of Jin Li was supported by Natural Science Foundation of Hebei Province (Grant No. A2019209533).

References

[1] N. A. Kudryashov and D. I. Sineshchikov, "Analytical solutions of a nonlinear convection-diffusion equation with polynomial sources," *Modelirovanie i Analiz Informatsionnykh Sistem*, vol. 23, no. 3, pp. 309–316, 2016.

[2] H. Wang, B. Shi, H. Liang, and Z. Chai, "Finite-difference lattice Boltzmann model for nonlinear convection-diffusion equations," *Applied Mathematics and Computation*, vol. 309, pp. 334–349, 2017.

[3] R. Eymard, T. Gallonet, and R. Herbin, "Error estimate for approximate solutions of a nonlinear convection-diffusion problem," *Advances in Differential Equations*, vol. 7, no. 4, pp. 419–440, 2002.

[4] J. D. Frutos, B. G. Archilla, and J. Novo, "Nonlinear convection-diffusion problems: fully discrete approximations and a posteriori error estimates," *IMA Journal of Numerical Analysis*, vol. 31, no. 4, pp. 1402–1430, 2011.

[5] A. Mohebbi and M. Dehghan, "High-order compact solution of the one-dimensional heat and advection–diffusion equations," *Applied Mathematical Modelling*, vol. 34, no. 10, pp. 3071–3084, 2010.

[6] N. R. Bayramov and J. K. Kraus, "On the stable solution of transient convection-diffusion equations," *Journal of Computational and Applied Mathematics*, vol. 280, pp. 275–293, 2015.

[7] J. Shen, T. Tang, and L. Wang, "Algorithms, analysis and applications," *Spectral Methods*, vol. 41, 2011.

[8] J. P. Berrut, S. A. Hosseini, and G. Klein, "The linear barycentric rational quadrature method for Volterra integral equations," *SIAM Journal on Scientific Computing*, vol. 36, no. 1, pp. 105–123, 2014.

[9] P. Berrut and G. Klein, "Recent advances in linear barycentric rational interpolation," *Journal of Computational and Applied Mathematics*, vol. 259, no. Part A, pp. 95–107, 2014.

[10] E. Cirillo and K. Hormann, "On the Lebesgue constant of barycentric rational Hermite interpolants at equidistant nodes," *Journal of Computational and Applied Mathematics*, vol. 349, pp. 292–301, 2019.

[11] A. Abdi, J.-P. Berrut, and S. A. Hosseini, "The linear barycentric rational method for a class of delay Volterra integro-differential equations," *Journal of Scientific Computing*, vol. 75, pp. 1757–1775, 2018.

[12] P. Berrut, M. S. Floater, and G. Klein, "Convergence rates of derivatives of a family of barycentric rational interpolants," *Applied Numerical Mathematics*, vol. 61, no. 9, pp. 989–1000, 2011.

[13] J. Li and Y. Cheng, "Linear barycentric rational collocation method for solving second-order Volterra integro-differential equation," *Computational and Applied Mathematics*, vol. 39, no. 2, 2020.

[14] J. Li and Y. Cheng, "Numerical solution of Volterra integro-differential equations with linear barycentric rational method," *International Journal of Applied and Computational Mathematics*, vol. 6, no. 5, p. 137, 2020.

[15] M. S. Floater and H. Kai, "Barycentric rational interpolation with no poles and high rates of approximation," *Numerische Mathematik*, vol. 107, no. 2, pp. 315–331, 2007.

[16] G. Klein and J. P. Berrut, "Linear rational finite differences from derivatives of barycentric rational interpolants," *SIAM Journal on Numerical Analysis*, vol. 50, no. 2, pp. 643–656, 2012.

[17] G. Klein and J.-P. Berrut, "Linear barycentric rational quadrature," *BIT Numerical Mathematics*, vol. 52, no. 2, pp. 407–424, 2012.

[18] J. Li and Y. Cheng, "Linear barycentric rational collocation method for solving heat conduction equation," *Numerical Methods for Partial Differential Equations*, vol. 37, no. 1, pp. 533–545, 2021.

[19] J. Li and Y. Cheng, "Barycentric rational method for solving biharmonic equation by depression of order," *Numerical Methods for Partial Differential Equations*, vol. 37, no. 3, pp. 1993–2007, 2021.

[20] J. Li, X. Su, and J. Qu, "Linear barycentric rational collocation method for solving telegraph equation," *Mathematical Methods in the Applied Sciences*, vol. 44, no. 14, pp. 11720–11737, 2021.

[21] J. Li and Y. Sang, "Linear barycentric rational collocation method for beam force vibration equation," *Shock and Vibration*, vol. 2021, Article ID 5584274, 11 pages, 2021.

[22] S. Li and Z. Wang, *High Precision Meshless barycentric Interpolation Collocation Method–Algorithmic Program and Engineering Application*, Science Publishing, 2012.

[23] Z. Wang and S. Li, *Barycentric interpolation collocation method for nonlinear problems*, National Defense Industry Press, 2015.

[24] Z. Wang, Z. Xu, and J. Li, "Mixed barycentric interpolation collocation method of displacement-pressure for incompressible plane elastic problems," *Chinese Journal of Applied Mechanics*, vol. 35, no. 3, pp. 195–201, 2018.

[25] Z. Wang, L. Zhang, Z. Xu, and J. Li, "Barycentric interpolation collocation method based on mixed displacement-stress formulation for solving plane elastic problems," *Chinese Journal of Applied Mechanics*, vol. 35, no. 2, pp. 304–309, 2018.